



Role of the photopolymerisation conditions in the broadening of the temperature range of the 'blue phases'

Igor Gvozдовskyy

To cite this article: Igor Gvozдовskyy (2016) Role of the photopolymerisation conditions in the broadening of the temperature range of the 'blue phases', *Liquid Crystals*, 43:12, 1813-1830, DOI: [10.1080/02678292.2016.1213431](https://doi.org/10.1080/02678292.2016.1213431)

To link to this article: <http://dx.doi.org/10.1080/02678292.2016.1213431>



Published online: 25 Jul 2016.



Submit your article to this journal [↗](#)



Article views: 105



View related articles [↗](#)



View Crossmark data [↗](#)

Role of the photopolymerisation conditions in the broadening of the temperature range of the 'blue phases'

Igor Gvozдовskyy

Department of Optical Quantum Electronics, Institute of Physics of the National Academy of Sciences of Ukraine, Kyiv, Ukraine

ABSTRACT

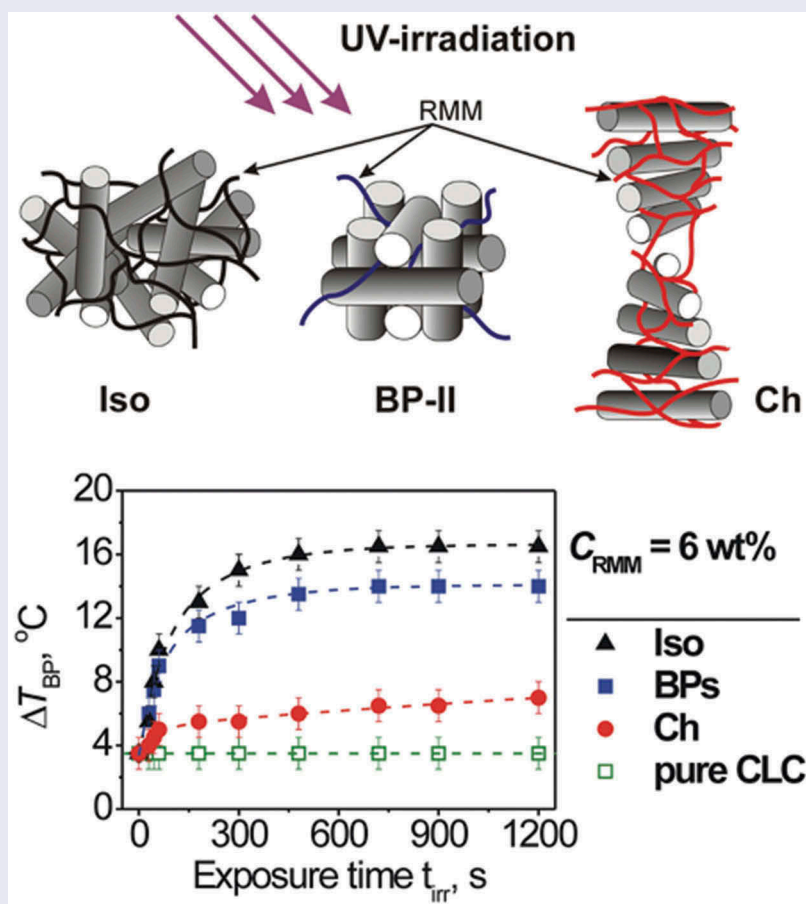
The influence of the photopolymerisation conditions during the formation of the blue phases (BPs) of the polymer-stabilised liquid crystal is reported. The reactive mesogen monomers (RMM) with various concentrations were added to the highly chiral thermotropic liquid crystal, which initially possesses a narrow temperature range of the existence of the BPs. The formation of the blue phases of the polymer-stabilised cholesteric liquid crystals (BP PSCLCs), containing cross-linking monomers without any photoinitiators, during their photopolymerisation in various phases (isotropic, BPs and cholesteric phase (Ch)), was independently studied in a relatively recent manuscript, published by H-Y Chen, et. al. *Liq. Cryst.*, 2016. doi:10.1080/02678292.2016.1173244. In the present studies, the concentration dependencies of the RMM and the influence of the exposure time during the photopolymerisation process on the broadening of the temperature range and spectral features of the BPs were examined. Under certain experimental conditions, a maximal broadening of the temperature range of the existence of the BPs after the photopolymerisation process of cross-linking monomers carried out in the isotropic phase (Iso) not in the BP or the Ch was found.

ARTICLE HISTORY

Received 13 April 2016
Accepted 12 July 2016

KEYWORDS

Blue phases;
polymer-stabilised
cholesteric liquid crystal;
chirality; phase transitions



Introduction

It is known that for certain cholesteric liquid crystals (CLCs) with a helix pitch $P < 5000 \text{ \AA}$ [1,2] the transition in a narrow temperature range between the cholesteric phase (Ch) and isotropic phase (Iso) can sometimes occur through a series of additional transitions of the self-assembled three-dimensional photonic crystal structures, well known as three thermodynamically stable ‘blue phases’ (BP-III, BP-II and BP-I). [3–10] Structures of BPs can be described as ‘double twist’ cylinders, where the director twists simultaneously in two independent directions, filling up large volumes of the three-dimensional space. Between the ‘double twist’ cylinders, there are line defects (disclinations), forming a cubic lattice. A local cubic lattice structure in the director field is observed for amorphous BP-III or the so-called fog BP, while BP-II and BP-I have a fluid three-dimensional periodic structure with the simple cubic and body-centred cubic symmetry, respectively. [7–12] It is an established fact that the periods of lattices of BP-II and BP-I are comparatively of the order of the visible wavelength region and due to this, the selective Bragg diffraction is observed. It is also known that BPs are optically active but, unlike Ch, they are optically isotropic and are not birefringent. [1,7–10,13–15]

The fact that the BPs of pure CLCs have the thermal stability in a very narrow temperature range (usually it is few degrees Celsius [8,9,13–15]) significantly limits their practical applications such as displays, optical filters, 3D lasers, *etc.* There are different methods to extend the temperature range ΔT_{BP} of BPs, based on the fabrication of new materials containing CLCs and polymers (the so-called blue phase of polymer-stabilised cholesteric liquid, crystals (BP PSCLCs) [16–20]); the synthesis of new molecules and liquid crystalline compounds [21–25] or the creation of BP polymer-templated nematic (BPTN) [26,27] lead to the increasing interest in their different applications: solution of the storage problems, [17–19] existence of BPs at room temperature [16,21,26–28] and essential extending of BPs thermal range. [21–24,27–37] It was also shown that guest components, namely polymers [16,26–32] or colloidal particles, [35,36,38] could form specific networks in BPs, by filling defect regions with high energy. [29] These networks can stabilise disclinations in a three-dimensional cubic lattice and reduce the free energy of BPs, owing to this fact, the temperature range (ΔT_{BP}) of the phase can extend. [39–42] The usage of BP PSCLCs is promising for photonics, including 3D lasers, [20,43–45] tunable gratings, [46] and displays. [33,47–51]

As can be seen from [16–20,26–33] usually BP PSCLCs are forming in a bulk of liquid crystals (LCs) by *in situ* photopolymerisation of the reactive mesogen monomers (RMM) along the disclinations in BPs. Recently it was shown that the optical and electro-optical behaviours of the optically isotropic chiral liquid crystalline composites, containing high concentrations of various monomers, could depend on temperature of the composite [51] or phase, wherein composites prepared by *in situ* photopolymerisation of cross-linking RMMs (notably in Iso or BPs). [42,52] Recently, the influence of various conditions of UV irradiation (*e.g.* wavelength, intensity, exposure time t_{irr} and temperature during polymerisation T_{irr}), composition of PSCLCs, concentration ratio of photo-initiators and RMM on electro-optical properties of BP PSCLCs and the extension of the temperature range ΔT_{BP} of BPs was studied in [31,42,52–57]. It was also shown that the electro-optical features (changes of the birefringence, chiral pitch and the Kerr constant), formation of the lattice BP (*i.e.* heterogeneous lattice generation or homogeneous lattice growth) and polymer stabilisation of BP PSCLCs (with only BP-I), containing high concentrations of various monomers, could sufficiently depend on different cooling rates and critical temperature in the phase transition of BP-I PSCLCs and BP-III PSCLCs. [42,56] However, until recently the comparison studies of the influence of photopolymerisation conditions of RMM (*e.g.* the temperature regime T_{irr} and exposure time t_{irr}) for all phases of CLC (*i.e.* Iso, BPs and Ch) on the broadening of BPs temperature range almost have not been reported. But it should be noted that the influence of the different photopolymerisation process (in Iso, BPs and Ch) under the formation of the polymer networks on the substrate by means of studies of their morphology with the aim to increase the thermal stability of BPs was recently reported in [58].

In this manuscript, the method of the extension of the temperature range of BPs will be experimentally demonstrated on a model based on a pure CLC, initially having a narrow ΔT_{BP} of BPs, with adding various concentrations of RMM without any photoinitiators, which are traditionally used in practice for the preparation of typical PSCLCs. Here, photopolymerisation of the composites, carried out in different phases (*i.e.* Iso, BPs and Ch), was studied independently with respect to the recently described analogous investigations in [58]. The obtained experimental results are in a good agreement with recent reports [42,53–58] and clearly show the importance of taking into consideration the photopolymerisation conditions of RMM (*i.e.* temperature regime T_{irr} during of photopolymerisation process,

exposure time t_{irr} at the formation of polymer network during UV exposure) to extend or control value of the temperature range ΔT_{BP} of BP PSCLCs.

Experiment

At the beginning, a pure highly chiral thermotropic liquid crystal was prepared. The non-mesogen right-handed chiral dopant (ChD) ZLI-3786 (R-811), obtained by Licrystal (Merck, Darmstadt, Germany), was used to prepare the pure CLC. ChD R-811 was dissolved at concentration $C = 30$ wt.% in the thermotropic nematic host MLC-6012 (E. Merck Ltd, Darmstadt, Germany). The clear temperature of the nematic MLC-6012 is $T_c = 86^\circ\text{C}$.

To study the influence of the photopolymerisation conditions on the extension of ΔT_{BP} of BPs, the cross-linker reactive mesogen monomers RMM-141 (Merck, Darmstadt, Germany) in various doping concentrations ($C_{\text{RMM}} = 3, 6, 10$ and 13 wt.%) was dissolved in the pure CLC. These mixtures were filled into LC cells in Iso at temperature $T = 56^\circ\text{C}$.

LC cells were made from two glass substrates covered with polyimide films for the strongly planar alignment. As was described early in [59], to obtain the planar alignment of the pure CLC, the solution of polymer oxidianiline-polyimide (ODAPI, Kapton synthesised by I. Gerus, Institute of Bio-organic Chemistry and Petrochemistry, NAS of Ukraine) was spin-coated on glass substrates and further annealed at temperature 240°C . Thereafter, substrates with thin films were unidirectionally rubbed. Thicknesses of the gap of LC cells were set to $d = 25.4 \pm 0.5 \mu\text{m}$ by Mylar spacer and measured by the interference method using the transmission spectra of empty cells.

To obtain PSCLC cross-linked polymer networks, illumination of the LC cells containing composite with certain C_{RMM} was carried out by UV lamp with the maximum wavelength $\lambda = 365$ nm. The power of the UV radiation $\lambda = 365$ nm was 6 W.

In order to study the influence of the photopolymerisation conditions on the broadening of ΔT_{BP} of BPs, the illumination of LC samples was carried out under various phases of mixture, namely in Iso at $T_{\text{irr}} = 56^\circ\text{C}$, BPs at $T_{\text{irr}} = 49^\circ\text{C}$ and Ch at $T_{\text{irr}} = 24^\circ\text{C}$.

The thermal phase diagrams of the pure CLC and the composites, containing various C_{RMM} , were studied during the cooling process of LC cells by using polarising microscopy. The LC textures were viewed through a polarising microscope BioLar (PZO, Warszawa, Poland) equipped with a digital camera Nikon D80 (Japan). The LC cells were placed in a thermostable heater, based on a temperature regulator MikRa 603

(LLD 'MikRa', Kyiv, Ukraine), and the accuracy of the temperature measurement was $\pm 0.1^\circ\text{C}$. The speed of the temperature change was $0.01^\circ\text{C}/\text{min}$ (0.1°C per 10 min).

In case of BP PSCLCs, when supercooled BP-I was observed, the LC cell additionally had undergone a 100 g-weight pressure with a value about ~ 3300 N/ m^2 . This procedure is necessary to check the correctness of determination of the temperature range ΔT_{BP} of BPs by using a polarising microscope. In the case, where no BP \rightarrow Ch transition is observed, the temperature slowly decreased again.

To record the transmission spectra of different phases (Iso, BPs and Ch) at a constant temperature, UV-VIS spectrophotometer (made at the Institute of Physics, Ukraine) was used. Spectra were recorded as a function of wavelength over a range of 400 – 700 nm, during slow cooling with rates $0.01^\circ\text{C}/\text{min}$, starting from Iso just above T_c ($T = 56^\circ\text{C}$) and finishing to Ch ($T = 24^\circ\text{C}$) with the selective reflection in the visible region.

Results and discussion

3.1. BPs of the pure CLC

At the beginning, to demonstrate the influence of the photopolymerisation conditions on the extension of ΔT_{BP} of BPs, the pure CLC, consisting of 30 wt.% right-handed ChD R-811 and 70 wt.% nematic liquid crystal MLC-6012, and possessing BPs within a narrow temperature range ΔT_{BP} , was chosen. It is found that the pure CLC had a clear temperature $T_c \sim 53^\circ\text{C}$, and during the cooling process of Iso, BPs existed within the temperature range $\Delta T_{\text{BP}} \sim 3.5^\circ\text{C}$, as schematically shown in Figure 1(a). Sequence phase transitions of the pure CLC are Iso 52°C BPs 48.5°C Ch. In addition, a small hysteresis during the heating of Ch ($\Delta T_{\text{BP}} \sim 2.8^\circ\text{C}$) is observed.

The textures of the typical phase transitions during the cooling of the sample from Iso to Ch with a slow cooling ratio $0.01^\circ\text{C}/\text{min}$ are shown in Figure 1(b). The sequence changes of the transmission spectrum, when one phase changes into another for the pure CLC, are shown in Figure 2. For Iso at temperature $T = 53^\circ\text{C}$ (Figure 1(i)) the transmission spectrum 1 is a horizontal line as shown in Figure 2(a). The transmittance value of Iso is ~ 95 – 98% . At temperature $T = 52^\circ\text{C}$, BP-III (fog BP) with 'island' texture is appeared (Figure 1(ii)). The transmission of the sample (Figure 2(a), spectrum 2) is very weak in the broad wavelength range 400 – 580 nm and fits the spectrum of the fog BP. [5,59] The decrease in sample temperature

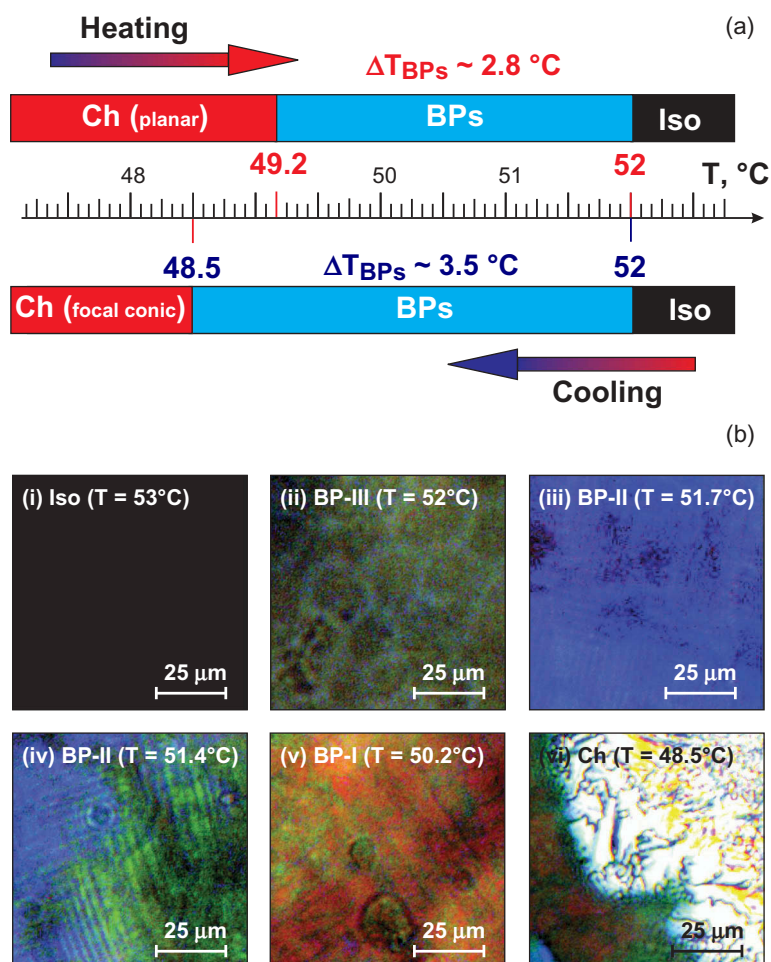


Figure 1. (Colour online) ‘Blue’ phases of the pure CLC, based on 30 wt.% right-handed chiral dopant R-811, dissolved in the nematic host MLC-6012. (a) Schematic diagrams of the sequence of phase transitions on heating and cooling of the pure CLC. (b) Microphotographs of textures of sequential phase transitions between Iso and Ch on cooling of the pure CLC: (i) Iso at 53°C; (ii) ‘island’ texture of BP-III at 52°C; ‘parquet’ textures of BP-II - (iii) with the uniform blue colour at 51.7°C, (iv) with the uniform green/blue colour at 51.4°C; and (v) with the uniform red colour at 50.2°C; and (vi) focal conic texture of Ch at 48.5°C. Thickness of the LC cell was $25.4 \pm 0.5 \mu\text{m}$. The cooling rate of the LC sample was $0.01^\circ\text{C}/\text{min}$.

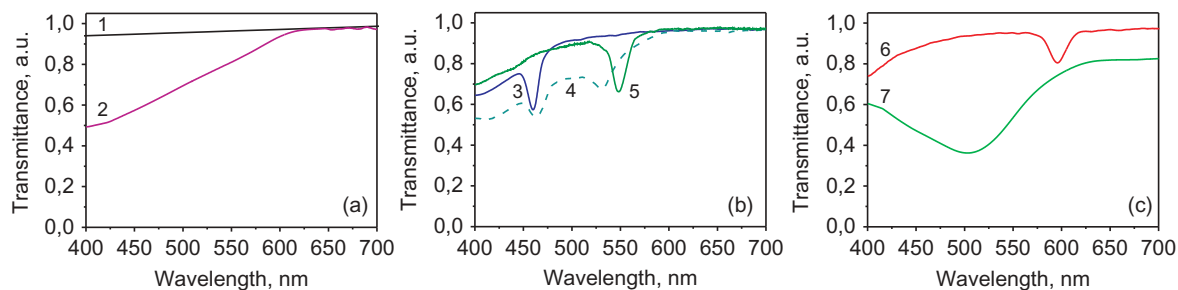


Figure 2. (Colour online) Transmission spectra of the pure CLC formed with 30 wt.% of R-811 added to the nematic host MLC-6012 at various values of the sample temperature: (a) Iso at 53°C (spectrum 1) and BP-III at 52°C (spectrum 2); (b) BP-II: at $T = 51.7^\circ\text{C}$ (spectrum 3) and at $T = 51.4^\circ\text{C}$ (spectra 4 and 5); and (c) BP-I at 50.2°C (spectrum 6) and the focal conic texture of Ch at 48.5°C (spectrum 7). Thickness of the LC cell was $25.4 \pm 0.5 \mu\text{m}$. The cooling rate of the sample was $0.01^\circ\text{C}/\text{min}$.

to $T = 51.7^\circ\text{C}$ leads to BP-III→BP-II transition with the appearance of the ‘parquet’ texture with the reflected uniform blue colour that covers the whole area of the cell (Figure 1(iii)).

As can be seen from Figure 1(iv), the ‘parquet’ texture with the reflected uniform green colour of BP-II at temperature $T = 51.4^\circ\text{C}$ is appeared. While cooling BP-II to $T = 51.4^\circ\text{C}$, the reflected colour which

changes from blue to green is observed with a polarising microscope and recorded with a spectrophotometer, as shown in Figure 2 (b, spectrum 4). As can be seen from Figure 2(b), transmission spectra 3–5 correspond to BP-II ‘parquet’ textures with the reflected uniform blue, blue/green and green colour, respectively. At a temperature of 50.2°C, the transition between BP-II and BP-I is observed (Figure 1(v)). As can be seen from Figure 2(c, spectrum 6), for the cooled BP-I, the maximum of the Bragg reflection is shifted into the red region of the visible spectrum. When the cell temperature decreases to $T = 48.5^\circ\text{C}$, the focal conic texture of Ch is observed. The texture of Ch and spectrum of the Bragg reflection are shown in Figure 1 (vi) and Figure 2(c, spectrum 7), respectively.

3.2. BPs of the non-irradiated PSCLC

The characteristic features of BP of the composites were initially studied without the photopolymerisation process. Here, in the sequel, the phase diagrams that can appear between BP-III and BP-II, BP-II and BP-I will not be discussed. As it was early studied in [30,31,39–41,52,57], here, in order to investigate the influence of the guest component (*i.e.* RMM without any photoinitiators) on the extension of ΔT_{BP} of BPs, various concentrations of RMM ($C_{\text{RMM}} = 3, 6, 10$ and 13 wt.%) were added to the pure CLC, hereby by forming various mixtures of the non-irradiated PSCLCs. The phase diagrams during the cooling and heating processes of non-irradiated composites, containing various C_{RMM} , are shown in Table 1.

As can be seen from diagrams in Table 1, during the cooling of Iso of the non-irradiated composites the temperature range ΔT_{BP} of BPs were within a range of $\sim 3.5\text{--}3.8^\circ\text{C}$, while during the heating of Ch, a small hysteresis was observed and ΔT_{BP} was $\sim 2.8\text{--}2.9^\circ\text{C}$, which is the same as for the case of the pure CLC (Figure 1(a)). These results lead to the conclusion that the extension of ΔT_{BP} of BPs slightly depends on concentration C_{RMM} of the non-irradiated PSCLCs. In addition, these results that are in

Table 1. The phase diagrams of non-irradiated PSCLCs, containing various concentrations of monomers, during the cooling and heating processes.

Concentration of RMM (wt.%)	Transition temperatures ($^\circ\text{C}$)	
	on cooling	on heating
3	Iso 52 BPs 48.3 Ch	Ch 49.2 BPs 52.1 Iso
6	Iso 51.9 BPs 48.3 Ch	Ch 49.2 BPs 52 Iso
10	Iso 52 BPs 48.2 Ch	Ch 49.1 BPs 51.9 Iso
13	Iso 51.9 BPs 48.4 Ch	Ch 49.1 BPs 52 Iso

the temperature measurement accuracy, are identical to results obtained in [29], when no diffractions of X-ray were observed for BP with iodised monomers without photopolymerisation.

It is also established that before UV irradiation of the composites, ‘parquet’ textures are always observed, as for the case of the pure CLC, shown in Figure 1 (b, (iii)–(v)). For example, the typical ‘parquet’ texture, observed under BP-III→BP-II transition of the pure CLC doping by 6 wt.% RMM, is shown in Figure 3.

In addition, spectral characteristics of BPs for the non-irradiated composites with various C_{RMM} (3, 6 and 13 wt.%), namely the full width at half minimum of the transmission spectrum (*i.e.* FWHM or $\Delta\lambda_{\text{FWHM}}$) and positions of the maximum of the wavelength of the selective Bragg reflection, are not changed in comparison with the spectral characteristics of BPs for the pure CLC. As can be seen from Figure 4 (a), at temperature $T = 51.6^\circ\text{C}$ (BP-II, blue colour of the ‘parquet’ texture), positions of the minimum transmittance (λ_{min}) are about $\sim 457 \pm 2$ nm and FWHM is about $\sim 10 \pm 2$ nm. At temperature $T = 51.3^\circ\text{C}$ (BP-II, green colour of the ‘parquet’ texture), $\lambda_{\text{min}} \sim 542 \pm 1$ nm and $\Delta\lambda_{\text{FWHM}}$ are in the range 10–17 nm, as can be seen in Figure 4(b). In the case of BP-I with the red colour of the ‘parquet’ texture (at $T = 50^\circ\text{C}$), values of λ_{min} and $\Delta\lambda_{\text{FWHM}}$ are 597 ± 3 nm and 19 ± 1 nm, respectively, as shown in Figure 4(c).

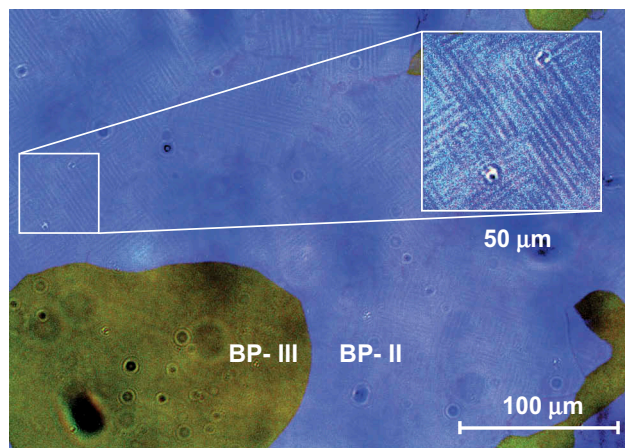


Figure 3. (Colour online) Microphotograph of BP-III→BP-II transition at 51.6°C during the cooling process of the non-irradiated PSCLC, containing 6 wt.% of RMM. The whole area of the LC cell is covered with the ‘parquet’ texture of the uniform blue colour. The inset depicts the ‘parquet’ texture in the enlarged scale, by having a higher image contrast. The rate of the temperature change was 0.01°C/min.

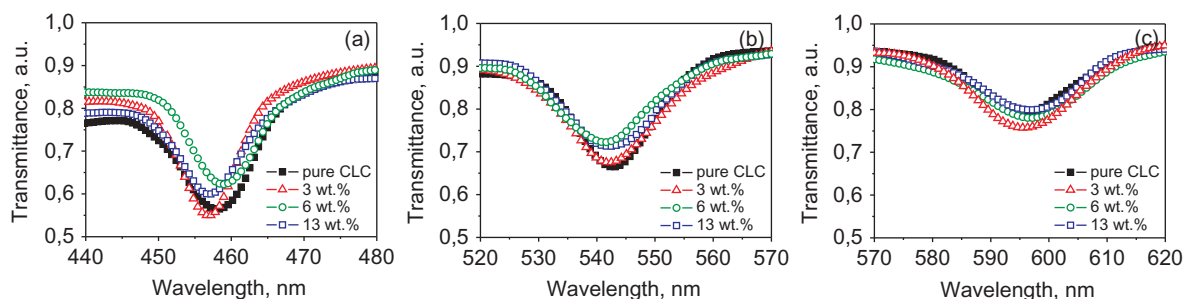


Figure 4. (Colour online) Transmission spectra of the pure CLC (solid squares), based on 30 wt.% of R-811 and 70 wt.% nematic MLC-6012 and non-irradiated PSCLCs, containing various concentrations of reactive mesogen monomers C_{RMM} : 3 wt.% (open triangles), 6 wt.% (open circles) and 13 wt.% (open squares) for: (a) BP-II: at $T = 51.6^\circ\text{C}$ (blue colour the ‘parquet’ texture, $\lambda_{\min} \sim 457 \pm 2$ nm and $\Delta\lambda_{FWHM} \sim 10 \pm 2$ nm), (b) BP-II: at $T = 51.3^\circ\text{C}$ (green colour the ‘parquet’ texture, $\lambda_{\min} \sim 542 \pm 1$ nm and $\Delta\lambda_{FWHM} \sim 10\text{--}17$ nm) and (c) BP-I at 50°C (red colour the ‘parquet’ texture, $\lambda_{\min} \sim 597 \pm 3$ nm and $\Delta\lambda_{FWHM} \sim 19 \pm 1$ nm). Thicknesses of LC cells were 25.4 ± 0.5 μm . The cooling rate of samples was $0.01^\circ\text{C}/\text{min}$.

3.3. BPs of the irradiated PSCLC

As mentioned below in [16–20,26–37,42,52–58], the temperature range ΔT_{BP} for stable BPs can be essentially extended to several tens of the degree Celsius by using *in situ* photopolymerisation of RMM in the bulk of the highly chiral liquid crystal in BPs. In this section, the influence of different photopolymerisation conditions on temperature transitions, broadening of the temperature range ΔT_{BP} of BPs and spectral characteristics of PSCLCs, containing various C_{RMM} , will be described.

Each time, prior to the photopolymerisation process, the composites, based on the pure CLC with certain C_{RMM} , were cooled to constant temperature T_{irr} , controlled by the thermostable heater. After this procedure, the photopolymerisation process was carried out with UV lamp ($\lambda_{\max} = 365$ nm) at the certain fixed exposure time t_{irr} . This irradiated mixture corresponds to PSCLC with certain properties being studied here.

In Tables 2–4, the phase diagrams on cooling after certain fixed time t_{irr} of UV exposure of PSCLCs, containing various C_{RMM} , are shown, when the photopolymerisation process was carried out in different phases of the composites, namely in Iso (at $T_{irr} = 56^\circ\text{C}$), BP (at $T_{irr} = 49^\circ\text{C}$) and Ch (at $T_{irr} = 24^\circ\text{C}$), respectively. By comparing the phase diagrams on cooling of the non-irradiated mixtures (Table 1) and the irradiated composites (in this case, PSCLCs) in different phases (Tables 2–4), following conclusions can be made. The temperature of Iso→BPs transition depends on the phase of photopolymerisation. As can be seen from Tables 2–4, the decrease in the photopolymerisation temperature (T_{irr}) leads to the decrease in the temperature of Iso→BPs transition that are in a good agreement with [42]. For example, in case of $C_{RMM} = 10$ wt.% and $t_{irr} = 300$ s, after the photopolymerisation process was carried out in: Iso (at 56°C , Table 2), BP (at 49°C , Table 3) and Ch (at 24°C ,

Table 2. The phase diagrams during the cooling process of PSCLCs, containing various concentrations of RMM, after UV irradiation at fixed exposure times ($t_{irr} = 30, 180, 300$ and 900 s) in Iso (at $T_{irr} = 56^\circ\text{C}$).

Concentration of RMM (wt.%)	Transition temperatures ($^\circ\text{C}$)			
	30 s	180 s	300 s	900 s
3	Iso 52.2 BPs 46.7 Ch	Iso 52.4 BPs 42.5 Ch	Iso 52.4 BPs 42.2 Ch	Iso 52.6 BPs 41.6 Ch
6	Iso 52.4 BPs 46.9 Ch	Iso 52.3 BPs 39.4 Ch	Iso 52.7 BPs 38.6 Ch	Iso 52.8 BPs 36.1 Ch
10	Iso 52.5 BPs 42.3 Ch	Iso 52.7 BPs 37.1 Ch	Iso 52.9 BPs 33.5 Ch	Iso 52.9 BPs 32.7 Ch
13	Iso 52.7 BPs 40.8 Ch	Iso 52.8 BPs 31.9 Ch	Iso 53 BPs 29.9 Ch	Iso 52.9 BPs 28.8 Ch

Table 3. The phase diagrams during the cooling process of PSCLCs, containing various concentrations of RMM, after UV irradiation at fixed exposure times ($t_{irr} = 30, 180, 300$ and 900 s) in BPs (at $T_{irr} = 49^\circ\text{C}$).

Concentration of RMM (wt.%)	Transition temperatures ($^\circ\text{C}$)			
	30 s	180 s	300 s	900 s
3	Iso 51.6 BPs 47.5 Ch	Iso 51.7 BPs 44.1 Ch	Iso 51.9 BPs 44.2 Ch	Iso 52.2 BPs 41.8 Ch
6	Iso 51.9 BPs 46 Ch	Iso 52.1 BPs 42 Ch	Iso 52.2 BPs 40.6 Ch	Iso 52.4 BPs 38.3 Ch
10	Iso 52.3 BPs 44.5 Ch	Iso 52.5 BPs 39.4 Ch	Iso 52.5 BPs 38 Ch	Iso 52.7 BPs 35.4 Ch
13	Iso 52.5 BPs 42.4 Ch	Iso 52.7 BPs 36.5 Ch	Iso 52.7 BPs 34.5 Ch	Iso 52.9 BPs 31.3 Ch

Table 4. The phase diagrams during the cooling process of PSCLCs, containing various concentrations of RMM, after UV irradiation at fixed exposure times ($t_{\text{irr}} = 30, 180, 300$ and 900 s) in Ch (at $T_{\text{irr}} = 24^\circ\text{C}$).

Concentration of RMM (wt.%)	Transition temperatures ($^\circ\text{C}$)			
	30 s	180 s	300 s	900 s
3	Iso 50.8 BPs 47.2 Ch	Iso 51.1 BPs 47.1 Ch	Iso 51.3 BPs 46.8 Ch	Iso 51.4 BPs 45.9 Ch
6	Iso 51.2 BPs 47.2 Ch	Iso 51.4 BPs 46 Ch	Iso 51.4 BPs 45.7 Ch	Iso 51.6 BPs 45.8 Ch
10	Iso 51.6 BPs 46.1 Ch	Iso 51.6 BPs 44.8 Ch	Iso 51.9 BPs 43.4 Ch	Iso 51.9 BPs 42.5 Ch
13	Iso 51.9 BPs 44.5 Ch	Iso 52.1 BPs 45.5 Ch	Iso 52.3 BPs 42.9 Ch	Iso 52.6 BPs 38.8 Ch

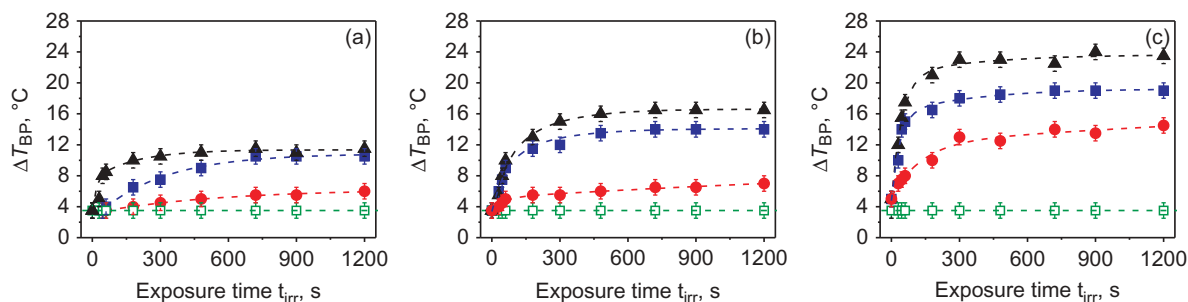
Table 4) temperature of Iso \rightarrow BPs transition were 52.9°C , 52.5°C and 51.9°C , respectively. In addition, as can be seen from Tables 2–4, for the irradiated mixtures with certain C_{RMM} and T_{irr} (or phase), temperature of Iso \rightarrow BPs transition insignificantly increases with the increase in the exposure time t_{irr} . The maximal shifts of temperature of Iso \rightarrow BPs transition were observed when the photopolymerisation process was carried out in Iso (for $C_{\text{RMM}} = 13$ wt.% at $t_{\text{irr}} = 300$ – 900 s). In addition, as can be seen from Tables 2–4, after UV exposure of the composites in different phases, the decrease in the temperature of BPs \rightarrow Ch transition and, hereupon, the broadening of the temperature range ΔT_{BP} of BPs is observed. These conclusions are in a certain agreement with [58].

In contrast to [42,56], where the authors determined critical temperature of the mixtures with high concentration of monomers and photoinitiators, here, because of the fact that the studied composites contain only certain concentrations of RMM without any photoinitiators, critical temperature has not been defined unfortunately.

The influence of UV exposure on the ΔT_{BP} of BPs for PSCLCs with various amounts of RMM ($C_{\text{RMM}} = 3, 6$ and 13 wt.%) is shown in Figure 5 (a), (b) and (c), respectively. During UV exposure of mixtures at constant temperatures in various phases (Iso at $T_{\text{irr}} = 56^\circ\text{C}$, BP at $T_{\text{irr}} = 49^\circ\text{C}$ and Ch at $T_{\text{irr}} = 24^\circ\text{C}$), the different extensions of ΔT_{BP} of BPs were observed. It is noted

that when the photopolymerisation process of the composites was carried out in Iso (at 56°C , triangle symbols) and Ch (at 24°C , circle symbols), maximal and minimal values of ΔT_{BP} of BPs were found, respectively. The surprising thing is that independently of RMM concentration, the extension of the temperature range ΔT_{BP} of BPs is observed after the photopolymerisation process carried out in Iso (Table 2 and Figure 5). It is obvious that different conditions of the photopolymerisation process to form the polymer networks will be mapped one-to-one onto their textures [58] and especially onto spectral characteristics of samples, as recently it was studied in [29], by investigating *in situ* photopolymerisation of cross-linking monomers in Iso and BPs of CLC, based on nematic 5CB (or the nematic mixture JC1041-XX) and ChD ZLI-4572, with high concentrations of RMM-257 and trimethylolpropane triacrylate (TMPTA).

It is obvious that the photopolymerisation process of RMM in Iso (without defects or disclinations) leads to the random formation of polymer networks in the depth of the LC cell through its entire thickness, owing to the isotropic (equivalent) growth of polymers in various directions, forming bead-like chains with a size of pores about 300 nm and less, as was recently shown in [58]. As can be seen from Figure 5 and Table 2, for these polymer networks, ΔT_{BP} of BPs is maximal for all concentrations of RMM. When the photopolymerisation process of PSCLCs was carried

**Figure 5.** (Colour online) Dependence of the temperature range ΔT_{BP} of BPs for PSCLCs, based on the pure CLC doped by RMM with various concentrations C_{RMM} : (a) 3 wt.%, (b) 6 wt.% and (c) 13 wt.%, on the exposure time t_{irr} at constant temperatures in different phases: Iso at $T_{\text{irr}} = 56^\circ\text{C}$ (solid triangles), BP at $T_{\text{irr}} = 49^\circ\text{C}$ (solid squares) and Ch at $T_{\text{irr}} = 24^\circ\text{C}$ (solid circles). The pure CLC (open squares), based on a right-handed ChD R-811, dissolved in the nematic host MLC-6012.

out in BPs (at 49°C, square solid symbols), a value of ΔT_{BP} of BPs is between values, obtained in Iso and Ch, as can be seen from Figure 5 and Table 3. As it is early described that before *in situ* the photopolymerisation process, RMM are situated randomly in BPs, while during photopolymerisation in BPs, the growing polymers drifted, segregated and the polymer cross-linking reaction occurs along disclination lines in three-dimensional directions by forming the polymer cubic network, [26,27] and the small-angle X-ray scattering (diffraction) was obtained, contrary to photopolymerisation in Iso and Ch, where no diffraction of X-ray was observed. [29]

In the case of photopolymerisation in Ch (at 24°C, circle symbols), the polymer network is forming along the director of quasinematic layers and along random disclinations in the highly chiral nematic. As it was described in [29], in both cases, molecules of RMM can drift to defects and grow along disclination lines. In this case, the polymer network is formed from disclinations embedded in between double twist cylinders, and this network has a cubic symmetry, [39–41] when PSCLCs were cooling to BPs. According to [58], when the photopolymerisation process has been carried out in Ch, the morphology of the polymer network is similar to ‘pine needles’ without closed pores that obviously leads to decrease in value of the temperature range ΔT_{BP} of BPs to zero. It was experimentally found that the polymer network in Ch leads to the extension of ΔT_{BP} of BPs in comparison with ΔT_{BP} range for the pure CLC, as it was predicted in [39–41]. However, the value of ΔT_{BP} is minimal, against the photopolymerisation process, carried out in Iso or BPs, as can be seen from Figure 5 and Table 4.

In addition, during photopolymerisation of RMM in different phases, the increase in exposure time t_{irr} also leads to the increase in the amount of cross-linking monomers through a depth of the LC cell (Figure 5), that is analogous to the investigation of the influence of the UV irradiation conditions (irradiation wavelength, intensity and exposure time) on hysteresis of voltage-dependent transmittance characteristics of BP PSCLCs, containing low concentrations monomers without any photoinitiators. [53] Obviously, owing to the fact that the prolonged UV exposure time t_{irr} of the composites leads to the decrease in a diameter of the pores, formed from polymer chains, as was shown in [58], the extension of the temperature range of ΔT_{BP} of BPs was observed, as shown in Figure 5 and Tables 2–4.

In addition, the increase in concentration of RMM in composites gives rise to the extension of ΔT_{BP} of BPs as can be seen from Figures 5 and 6. It is in a good agreement with results founded in [31], under

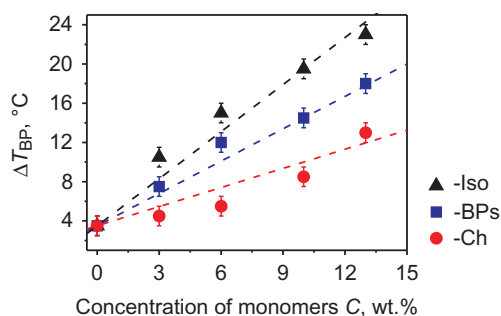


Figure 6. (Colour online) The concentration dependence of the extension of ΔT_{BP} of BPs of PSCLCs after the photopolymerisation process of RMM, carried out at the fixed exposure time $t_{irr} = 300$ s, in: Iso at 56°C (solid triangles), BP at 49°C (solid squares) and Ch at 24°C (solid circles).

the study of the influence of the polystyrene concentration for various molecular weights on the BP temperature ranges. Concentration dependencies of the temperature range of BPs after photopolymerisation of the composites at the fixed exposure time (e.g. $t_{irr} = 300$ s) are shown in Figure 6. As can be seen from linear dependencies, the increase in C_{RMM} results in the broadening of ΔT_{BP} . It can be explained on the basis of investigations reported in [55,58], where it is shown that during the cross-linking process monomers interconnect, increasing the chain length with further reducing of chain mobility in the polymer network that is important for the broadening of the temperature range.

Let us compare textures of PSCLCs formed at $T_{irr} = 56^\circ\text{C}$, 49°C and 24°C , as shown in Figure 7 (at $T = 53^\circ\text{C}$), Figure 8 (at $T = 49^\circ\text{C}$) and Figure 9 (at $T = 24^\circ\text{C}$), respectively. In Figures 7–9 each texture differs in both concentration of RMM or the photopolymerisation conditions (*i.e.* temperature T_{irr} and exposure time t_{irr}) during the cross-linking process of monomers. For instance, polymer networks were formed under UV irradiation of composite in different phases (*i.e.* in Iso at $T_{irr} = 56^\circ\text{C}$, BP at $T_{irr} = 49^\circ\text{C}$ and Ch at $T_{irr} = 24^\circ\text{C}$). In addition, polymer networks were formed for the composite containing certain concentration of RMM ($C_{RMM} = 3, 6$ and 13 wt.%). To compare the non-irradiated composite and irradiated textures of PSCLC, photographs for fixed exposition times $t_{irr} = 0$ and 180 s are shown in Figures 7–9.

Textures of PSCLCs at 53°C , containing various C_{RMM} , after UV exposure in different phases (Iso, BP and Ch) are shown in Figure 7. Contrary to the non-irradiated Iso (Figure 7 (a), (e) and (i)), a typical ‘granular’ texture appears after UV exposure, as can be seen from Figure 7 (b)–(d), (f)–(h) and (j)–(l). It is seen that an increase in C_{RMM} leads to decrease in the

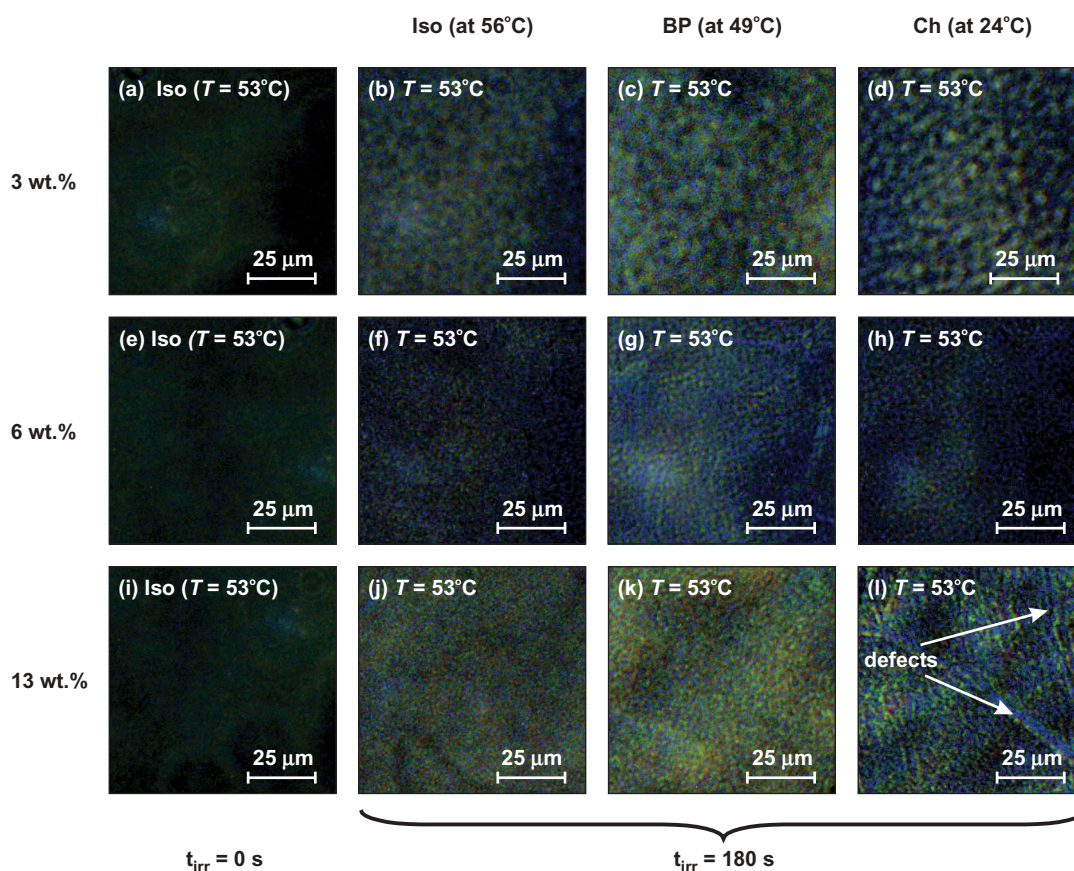


Figure 7. (Colour online) Photographs of textures at $T = 53^\circ\text{C}$ for PSCLCs, containing various concentrations of RMM-141: (a)–(d) for $C_{\text{RMM}} = 3$ wt.%, (e)–(h) for $C_{\text{RMM}} = 6$ wt.% and (i)–(l) for $C_{\text{RMM}} = 13$ wt.%. Photographs (a), (e) and (i) – non-irradiated textures of Iso at $T = 53^\circ\text{C}$ for PSCLCs, containing various concentrations of RMM. The ‘granular’ textures of PSCLCs (at $T = 53^\circ\text{C}$), when polymer networks were formed during UV exposure in: Iso at 56°C – (b), (f) and (j); BP at 49°C – (c), (g) and (k); and Ch at 24°C – (d), (h) and (l). UV irradiation was carried out at $\lambda_{\text{max}} = 365$ nm and exposure time $t_{\text{irr}} = 180$ s. Arrows show defects formed in places of oily streak defects after the photopolymerisation process in Ch ($T_{\text{irr}} = 24^\circ\text{C}$).

size of the ‘grain’. However, after UV exposure, carried out only in Ch (at 24°C), in the case of higher concentration of RMM ($C_{\text{RMM}} = 13$ wt.%), ‘granular’ textures together with defects formed in places of oily streak defects owing to the drift and segregation of the monomers, according to [40], are observed (Figure 7 (l)).

Figure 8 shows some typical textures of PSCLCs at temperature $T = 49^\circ\text{C}$, when the photopolymerisation process was carried out in different phases (*i.e.* in Iso at 56°C , BP at 49°C and Ch at 24°C) of the composites containing various C_{RMM} (3, 6 and 13 wt.%). It is worth mentioning that as in case of the pure CLC, the non-irradiated mixtures, containing various C_{RMM} , are structured so that the red colour ‘parquet’ texture of BP-I (at 49°C) is observed (Figure 8 (a), (e) and (i)). After UV exposures, carried out in different phases, the ‘platelet’ textures of BP-II of PSCLC, containing only 3 wt.% of RMM, are observed (Figure 8 (b), (c) and (d)).

In the case of higher C_{RMM} (*i.e.* for 6 and 13 wt.%), the monodomain texture of PSCLCs with the uniform colour against the background of the ‘granular’ texture is observed (Figure 8 (f)–(h) and (j)–(l)). But once the photopolymerisation process was carried out in Ch (at 24°C), additionally to the above described texture, the appearance of the defects, formed in places of oily streak defects, was also observed (Figure 8 (h) and (l)).

Textures of PSCLCs at 24°C , containing various C_{RMM} , before and after UV exposure in different phases (*i.e.* in Iso at $T_{\text{irr}} = 56^\circ\text{C}$, BP at $T_{\text{irr}} = 49^\circ\text{C}$ and Ch at $T_{\text{irr}} = 24^\circ\text{C}$) are shown in Figure 9. Before UV exposure of the composites, the typical planar texture together with oily streak defects, which are inherent in highly chiral thermotropic LCs, is shown in Figure 9 (a), (e) and (j).

As can be seen from Figure 9, once the photopolymerisation processes were carried in different phases, textures of PSCLCs at 24°C , containing various C_{RMM} , are diverge considerably. In case of low concentration

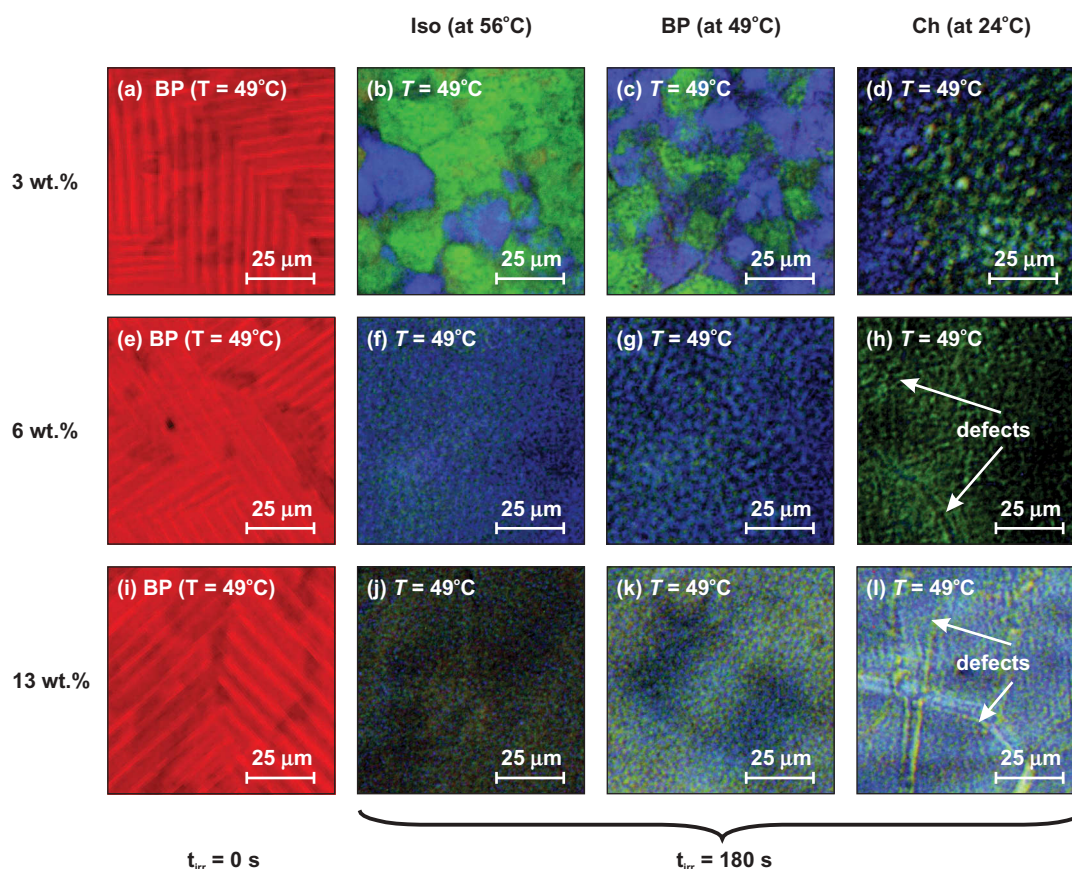


Figure 8. (Colour online) Photographs of textures at $T = 49^\circ\text{C}$ for PSCLCs, containing various concentrations of RMM-141: (a)–(d) for $C_{\text{RMM}} = 3 \text{ wt.}\%$, (e)–(h) for $C_{\text{RMM}} = 6 \text{ wt.}\%$ and (i)–(l) for $C_{\text{RMM}} = 13 \text{ wt.}\%$. Photographs (a), (e) and (i) – non-irradiated BPs of PSCLCs, containing various concentrations of RMM. Textures after UV irradiation of PSCLCs, when polymer networks were formed during UV exposure in: Iso at 56°C for (b), (f) and (j); BP at 49°C for (c), (g) and (k); and Ch at 24°C for (d), (h) and (l). UV irradiation was carried out at $\lambda_{\text{max}} = 365 \text{ nm}$ and the exposure time $t_{\text{irr}} = 180 \text{ s}$. Arrows show defects formed in places of oily streak defects after the photopolymerisation process in Ch ($T_{\text{irr}} = 24^\circ\text{C}$).

of RMM ($C_{\text{RMM}} = 3 \text{ wt.}\%$), the typical focal conic texture was observed, when the photopolymerisation process of the composite was carried out in Iso at 56°C and BP at 49°C . But, once UV exposure was carried out in Ch of the mixtures, containing various C_{RMM} , the ‘granular’ texture together with oily streak defects was observed (Figure 9 (d), (h) and (l)). Further, once the photopolymerisation processes of the composites, containing higher C_{RMM} (*i.e.* 6 and 13 wt.%), were carried out in Iso or BP, the uniformly distributed ‘granular’ textures of PSCLCs at 24°C were observed (Figure 9 (f), (g), (j) and (k)).

From the textures, observed in Figures 7–9, it may be concluded that during photopolymerisation of the composites in Iso (at $T_{\text{irr}} = 56^\circ\text{C}$), uniform textures of PSCLCs at 53°C , 49°C and 24°C were observed for various C_{RMM} . It can be assumed that the performance of photopolymerisation in Iso leads to the production of the random cross linking of monomers followed by the formation of polymer networks in medium without

defects and disclination lines. Due to this fact, as can be seen from Figure 5 (solid triangles), for PSCLCs, containing various C_{RMM} , the extension of ΔT_{BP} of BPs is maximal and increases with the rise of RMM concentration. In accordance with [29,39–41], it can be assumed that during photopolymerisation of the composites in BP (at $T_{\text{irr}} = 49^\circ\text{C}$), polymer cubic networks are formed in three-dimensional directions due to the cross-linking reaction that occurs along disclination lines, which are intrinsic in BPs. As can be seen from Figure 5 (solid squares), the extension of ΔT_{BP} of BPs, observed with the increasing C_{RMM} , is less than in Iso (medium without defects and disclination lines). As was found experimentally, the formation of polymer networks during UV exposure of Ch of the composites leads to the increase in the temperature range in comparison with the pure CLC, as shown in Figure 5 (solid circles and open squares, respectively). However, in this case, lower values of the extension of ΔT_{BP} of BPs are observed in comparison with photopolymerisation

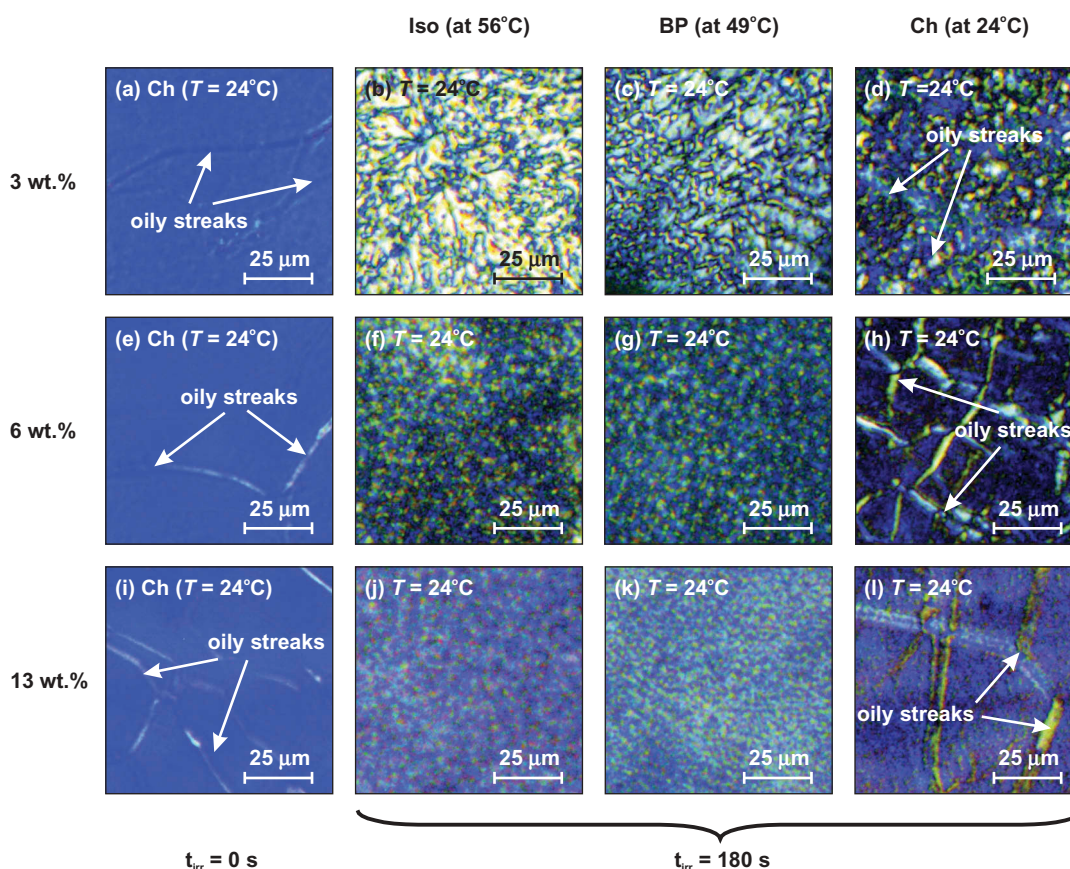


Figure 9. (Colour online) Photographs of textures at $T = 24^\circ\text{C}$ for PSCLCs, containing various concentrations of RMM-141: (a)–(d) for $C_{\text{RMM}} = 3$ wt.%, (e)–(h) for $C_{\text{RMM}} = 6$ wt.% and (i)–(l) for $C_{\text{RMM}} = 13$ wt.%. Photographs (a), (e) and (i) – non-irradiated BPs of PSCLCs, containing various concentrations of RMM. Textures after UV irradiation of PSCLCs, when polymer networks were formed during UV exposure in: Iso at 56°C for (b), (f) and (j); BP at 49°C for (c), (g) and (k); and Ch at 24°C for (d), (h) and (l). UV irradiation was carried out at $\lambda_{\text{max}} = 365$ nm and the exposure time $t_{\text{irr}} = 180$ s. Arrows show oily streak defects.

processes carried out in Iso and BP medium. It is obviously that the formation of stable chiral polymer networks (e.g. like ‘pine needles’, as shown in [58]) together with stable defects (e.g. stable oily streaks owing to the drift and segregation of monomers [41]) during UV exposure is a main reason for lower values of ΔT_{BP} of BPs, which are observed after photopolymerisation in Ch of the mixtures containing various C_{RMM} .

Obviously from Figures 7–9, it may be concluded that for PSCLCs, containing various C_{RMM} , the appearance of ‘granular’ textures, the change of the ‘grain’ size of the texture and the observation of different defects after UV exposure at constant temperature in different phases (or in other words during the photopolymerisation process) can cause the change of optical characteristics (in particular, spectral features) of BPs.

Below, qualitative analysis of the transmission spectra of BPs for PSCLCs with various C_{RMM} will be made, when the photopolymerisation processes were carried out in different phases (i.e. in Iso at 56°C , BP at 49°C

and Ch at 24°C). In Figures 10–12 are shown some transmission spectra of BPs of PSCLCs at fixed UV exposure times (i.e. $t_{\text{irr}} = 30, 180$ and 900 s).

Once UV exposure of the composites was carried out in different phases (Iso, BP and Ch) and PSCLCs was further cooled to the appearance of BPs, typical textures (by having analogy with Figure 8) of BPs, were observed. Transmission spectra of BPs of PSCLCs, formed in Iso, BP and Ch within the temperature range of the existence of BPs are shown in Figures 10–12, respectively.

As can be seen from Figures 10–12, the increase both in concentration of RMM and UV exposure time, during the photopolymerisation processes of PSCLCs in Iso, BP or Ch result in changes of the spectral characteristics of BPs of PSCLCs. It is noted that the increase in the concentration of RMM in the pure CLC also leads to the decrease in the transmittance of the sample and the broadening of transmission spectra $\Delta\lambda_{\text{FWHM}}$, as can be seen from Figures 10–12 (a), (d) and (g) and Figures 10–12 (d), (e) and (f),

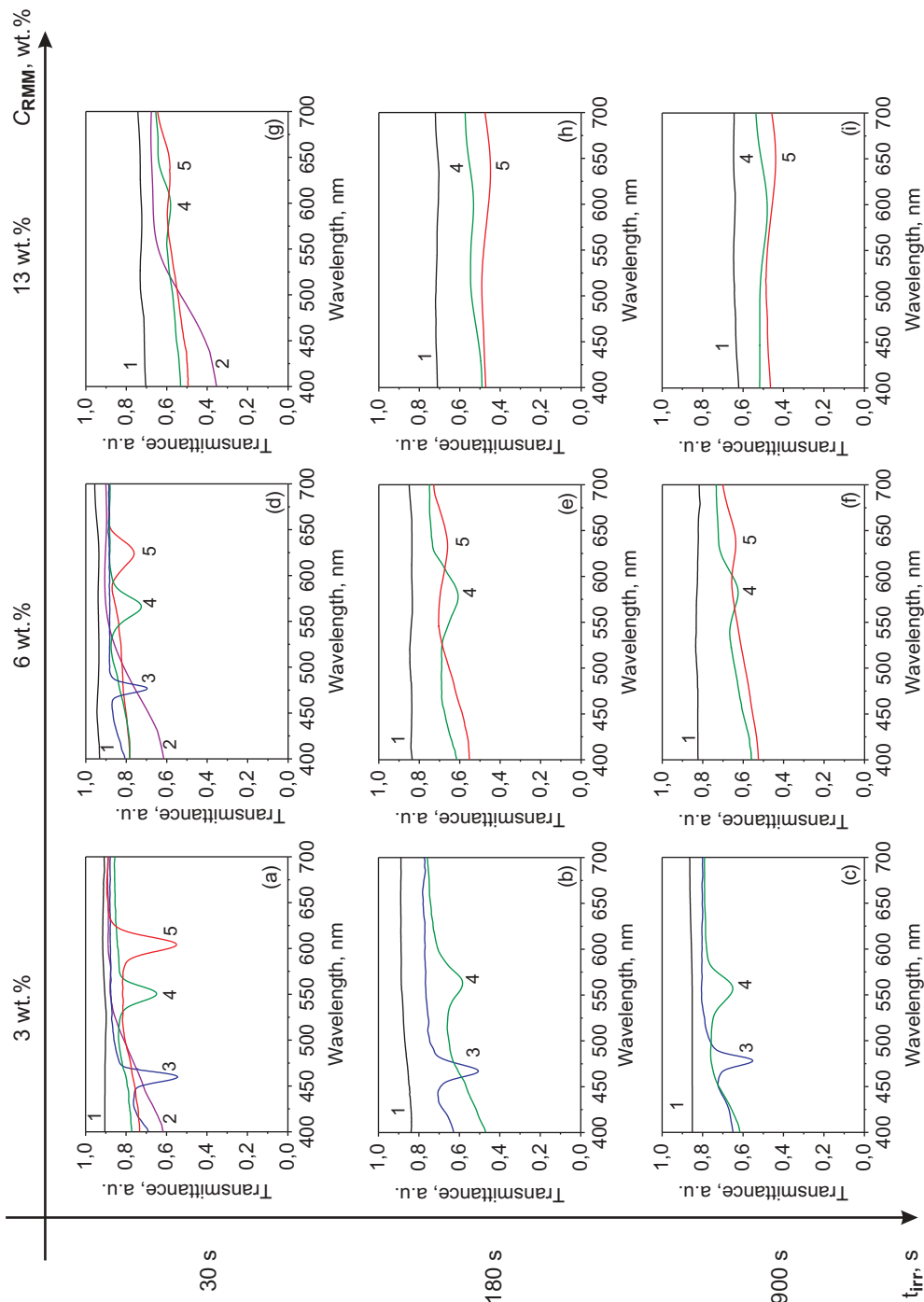


Figure 10. (Colour online) Transmission spectra of BPs of PSCLCs, formed with the pure CLC doped by various C_{RMM} : (a)–(c) – 3 wt.%; (d)–(f) – 6 wt.% and (g)–(i) – 13 wt.% after UV exposure in Iso at $T_{irr} = 56^\circ\text{C}$ over the course of t_{irr} : (a), (d) and (g) – 30 s; (b), (e) and (h) – 180 s; (c), (f) and (i) – 900 s and various values of the sample temperature T : Iso (spectrum 1) at 53°C – (a)–(i); BP-III (spectrum 2) at 51.8°C – (a), at 52.2°C – (d) and at 52.9°C – (g); BP-II (spectrum 3) at 51.1°C – (a), at 51.4°C – (d) and at 50.6°C – (b) and (c); BP-I (spectrum 4) at 50.4°C – (a), (d) and (g), at 47.5°C – (b) and (c) and at 42.5°C – (g), (e), (h), (f) and (i). Thicknesses of the LC cells were $25.4 \pm 0.5 \mu\text{m}$. The cooling rate of the sample was $0.01^\circ\text{C}/\text{min}$.

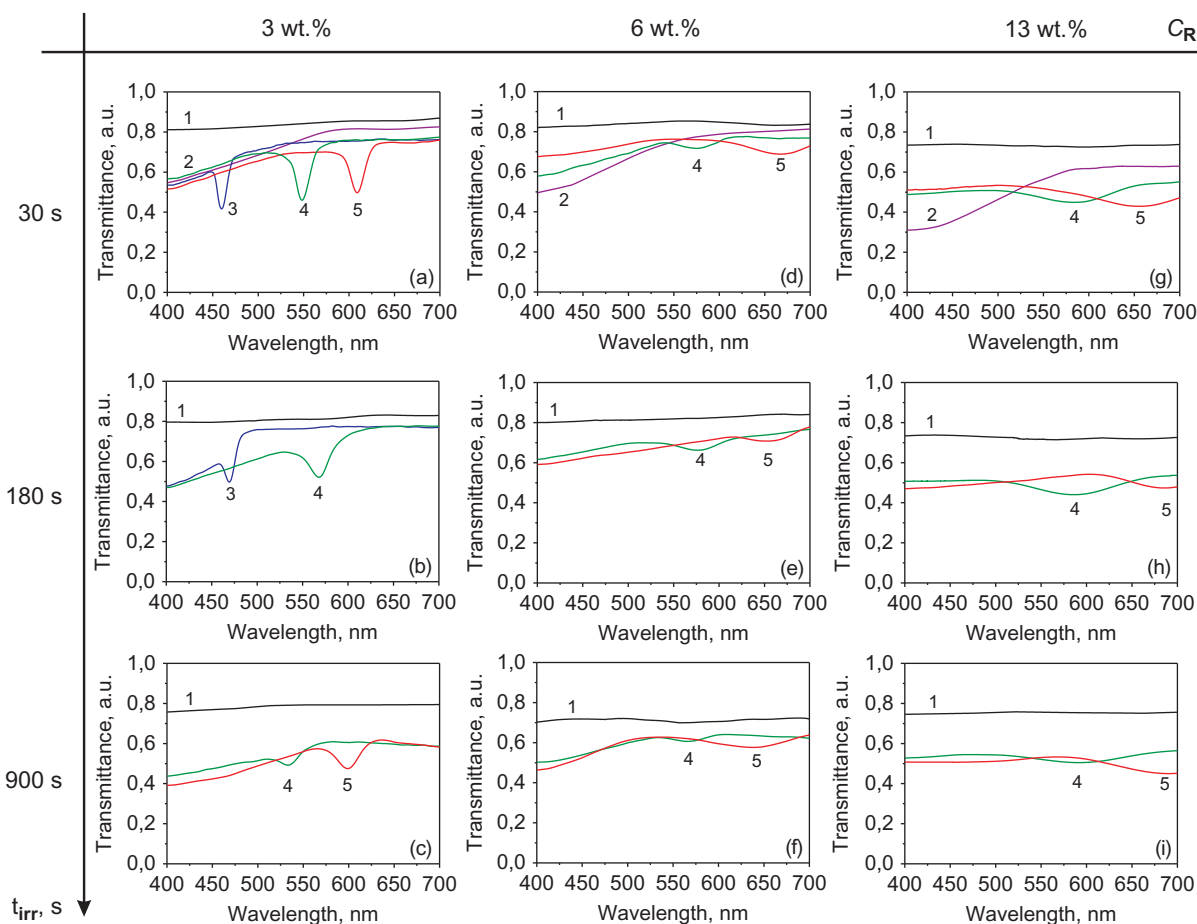


Figure 11. (Colour online) Transmission spectra of BPs of PSCLCs, formed with pure CLC doped by various concentrations of RMM C_{RMM} : (a)–(c) – 3 wt.%; (d)–(f) – 6 wt.% and (g)–(i) – 13 wt.% after UV exposure in BP at $T_{irr} = 49^\circ\text{C}$ over the course of t_{irr} : (a), (d) and (g) – 30 s; (b), (e) and (h) – 180 s; (c), (f) and (i) – 900 s and various values of the sample temperature T : Iso (spectrum 1) at 53°C – (a)–(i); BP-III (spectrum 2) at 51.4°C – (a), at 51.8°C – (d) and at 52.2°C – (g); BP-II (spectrum 3) at 50.8°C – (a) and (b); BP-II (spectrum 4) at 48.5°C – (a), (b) and (d) at 46°C – (e), (g) and (h) and at 40.5°C – (c), (f) and (i); BP-I (spectrum 5) at 48°C – (a) and (d), at 45.5°C – (c), (e), (g) and (h) and at 38.5°C – (f) and (i). Thicknesses of the LC cells were $25.4 \pm 0.5 \mu\text{m}$. The cooling rate of the sample was $0.01^\circ\text{C}/\text{min}$.

respectively. It can be assumed that the broadening of transmission spectra is related to the appearance of the ‘granular’ texture (or ‘granular’ textures together with defects) (Figure 7), observed after UV exposure, and also depends on the exposure time t_{irr} . In addition, the increase in C_{RMM} and duration of the exposure time t_{irr} give rise to the shift of the minimum of wavelength of the transmission spectrum λ_{min} (or wavelength of maximum of Bragg reflection λ_{max}), as can be seen from Figure 10, Figure 11 and Figure 12, by comparing spectra in columns (e.g. column (a)–(c) with column (d)–(f) or (g)–(i)) and rows (e.g. row (a), (d), (g) with row (b), (e), (h) or (c), (f), (i)), respectively.

For a rough comparison, let consider spectrum 4 depicted in Figures 10–12, as an example of the change of the position λ_{min} of transmittance and $\Delta\lambda_{FWHM}$ for various C_{RMM} and duration of the exposure time t_{irr} , when the photopolymerisation process was carried out

in different phases, in relation to these features of BPs of the pure CLC or non-irradiated composites, presented above in Figure 4. In the case of spectrum 4 from Figures 10–12, dependencies of maximal values of the shift of λ_{min} and $\Delta\lambda_{FWHM}$ as functions of the exposure time t_{irr} are shown in Figures 13 and 14, respectively.

As can be seen from Figure 13, for the pure CLC (depicted by number 1 with solid spheres) during UV exposure, no shift is observed, while for UV irradiated PSCLCs, the shifts of λ_{min} are observed both for various C_{RMM} (depicted by numbers 2–4 with open symbols) and for the photopolymerisation processes carried out in different phases, namely, in Iso at $T_{irr} = 56^\circ\text{C}$ (a), BP at $T_{irr} = 49^\circ\text{C}$ (b) and Ch at $T_{irr} = 24^\circ\text{C}$ (c). In addition, it is seen that the increase in C_{RMM} results in the increase in the value of shift of λ_{min} (Figure 13).

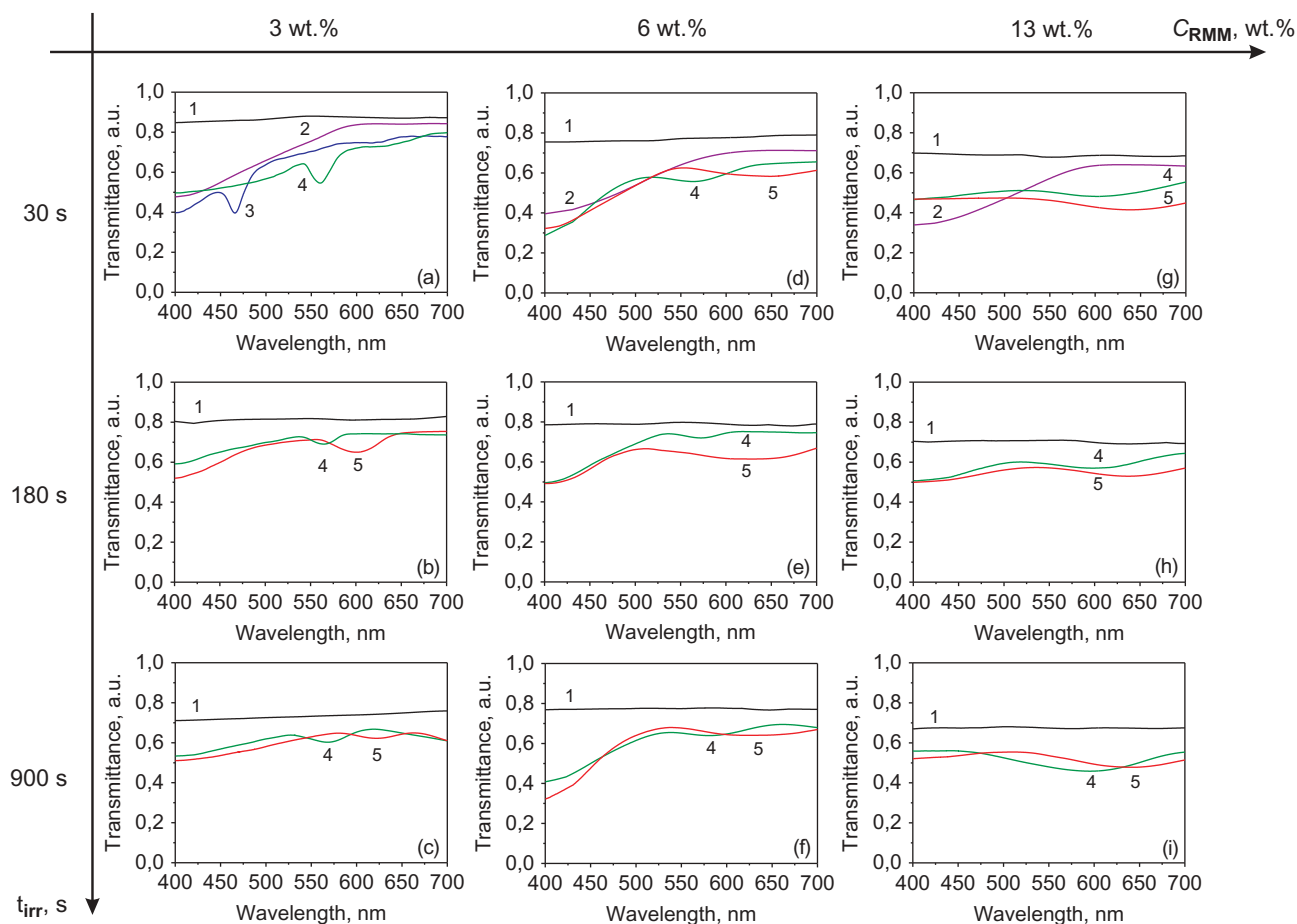


Figure 12. (Colour online) Transmission spectra of BPs of PSCLCs, formed with the pure CLC doped by various concentrations of RMM C_{RMM} : (a)–(c) – 3 wt.%; (d)–(f) – 6 wt.% and (g)–(i) – 13 wt.% after UV exposure in Ch at $T_{irr} = 24^\circ\text{C}$ over the course of t_{irr} : (a), (d) and (g) – 30 s; (b), (e) and (h) – 180 s; (c), (f) and (i) – 900 s and various values of the sample temperature T : Iso (spectrum 1) at 53°C – (a)–(i); BP-III (spectrum 2) at 50.6°C – (a) and at 51.1°C – (d); BP-II (spectrum 3) at 50.5°C – (a); BP-II (spectrum 4) at 49°C – (a)–(h) and at 45.5°C – (i); BP-I (spectrum 5) at 47.5°C (b)–(h) and at 42.5°C (i). Thickness of the LC cell was $25.4 \pm 0.5 \mu\text{m}$. The cooling rate of the sample was $0.01^\circ\text{C}/\text{min}$.

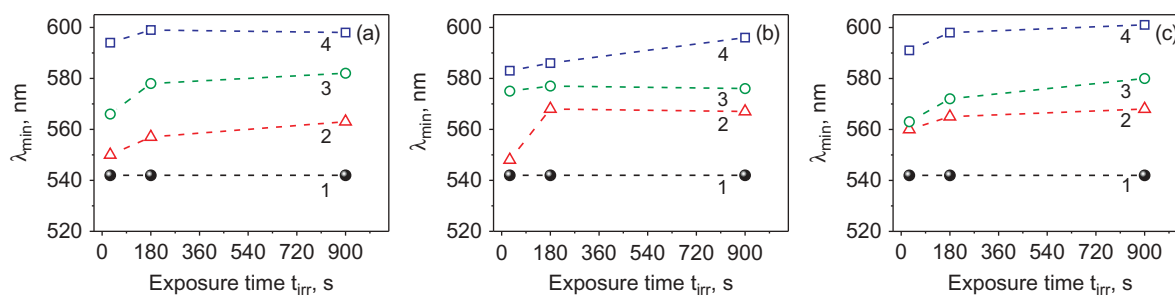


Figure 13. (Colour online) Dependence of minimum of the transmittance on the exposure time t_{irr} for BPs (spectrum 4), when the photopolymerisation process of PSCLCs was carried out in: (a) Iso at $T_{irr} = 56^\circ\text{C}$, (b) BP at $T_{irr} = 49^\circ\text{C}$ and (c) Ch at $T_{irr} = 24^\circ\text{C}$. The shift of λ_{min} denotes for the pure CLC (curve 1 with solid spheres) and PSCLCs, containing various C_{RMM} : 3 wt.% (curve 2 with open triangles), 6 wt.% (curve 3 with open circles) and 13 wt.% (curve 4 with open squares). The pure CLC was based on 30 wt.% R-811 dissolved in nematic MLC-6012. The cooling rate of the sample was $0.01^\circ\text{C}/\text{min}$.

As can be seen from **Figure 14**, the broadening of $\Delta\lambda_{FWHM}$ depends on C_{RMM} (depicted by numbers with solid symbols) and exposure time t_{irr} . In addition, the broadening of $\Delta\lambda_{FWHM}$, when the photopolymerisation

process of the composites was carried out in Iso at $T_{irr} = 56^\circ\text{C}$, BP at $T_{irr} = 49^\circ\text{C}$ and Ch at $T_{irr} = 24^\circ\text{C}$, is shown in **Figure 14** (a), (b) and (c), respectively. It is seen that in contrary to the non-irradiated mixtures

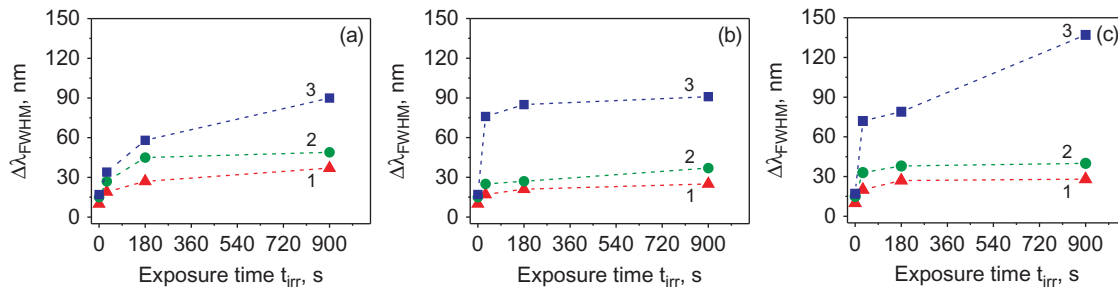


Figure 14. (Colour online) Dependence of broadening of $\Delta\lambda_{FWHM}$ on the exposure time t_{irr} for BPs (spectrum 4), when the photopolymerisation process of PSCLCs, containing various C_{RMM} : 3 wt.% (curve 1 with solid triangles), 6 wt.% (curve 3 with solid circles) and 13 wt.% (curve 4 with solid squares), was carried out in: (a) Iso at $T_{irr} = 56^\circ\text{C}$, (b) BP at $T_{irr} = 49^\circ\text{C}$ and (c) Ch at $T_{irr} = 24^\circ\text{C}$.

(Figure 4), for the irradiated composites the increase in value of $\Delta\lambda_{FWHM}$ is observed under all conditions of photopolymerisation (phase or so-called T_{irr} and the exposure time t_{irr}) (Figure 14). The minimal broadening of $\Delta\lambda_{FWHM}$ ($\sim 15\text{--}25$ nm) was observed in the case of $C_{RMM} = 3$ and 6 wt.% under all conditions of photopolymerisation (Figure 14 (a), (b) and (c), curves 1 and 2). However, when C_{RMM} is 13 wt.%, maximum values of $\Delta\lambda_{FWHM}$ ($\sim 30\text{--}140$ nm) are observed after UV exposure of composites in all phases, as can be seen from curves 3 of Figure 14 (a), (b) and (c). It is in a good agreement with the conclusion in [52], when the polymer network, formed in Iso, possesses weak spectral characteristics (*i.e.* no reflection peaks) of BPs of PSCLCs, containing a higher concentration ratio (more, than 13 wt.%) of various monomers. As can be seen from Figures 10–14, under any conditions of photopolymerisation, the usage of low C_{RMM} (3 and 6 wt.%) leads to the retention of reflection peaks of BPs of PSCLCs and also gives rise to the extension of ΔT_{BP} of BPs of PSCLCs, in comparison with the pure CLC (Figure 5).

After the photopolymerisation process of the composites, containing higher concentration of RMM ($C_{RMM} = 13$ wt.%), spectral characteristics of BPs are

strongly changed as was recently described in the case of Ch, having white reflection spectra, [60,61] or for BPs, having no reflection spectra after UV exposure in Iso. [52]

In addition, it was also found that the extension of ΔT_{BP} of BPs of PSCLCs could be controlled by the choice of the certain constant temperature T_{irr} wherein the photopolymerisation process of RMM takes place. By way of illustration, temperature dependencies of the extension of ΔT_{BP} for PSCLCs, formed during exposure time $t_{irr} = 300$ s and at different photopolymerisation temperatures T_{irr} in Iso (solid squares), BPs (solid circles) and Ch (solid triangles) and contained various C_{RMM} (3, 6 and 13 wt.%), are shown in Figures 15 (a), (b) and (c), respectively.

It is seen that the extension of temperature of BPs of PSCLCs, containing various C_{RMM} , is no dependent on temperature T_{irr} , when the photopolymerisation process was carried out in Iso and Ch. These results are analogous to those obtained in [42], where the stability of BP-III PSCLC also does not depend on temperature of photopolymerisation for the composition with certain concentration ratio of monomers. On the contrary, after photopolymerisation of the composites, carried out in BPs (*i.e.* BPs characterised by different

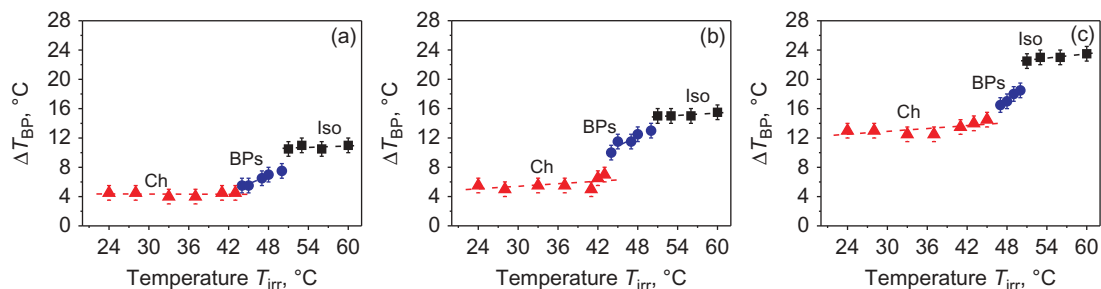


Figure 15. (Colour online) Dependence of the extension of ΔT_{BP} on constant temperatures T_{irr} wherein the photopolymerisation processes of PSCLCs, containing C_{RMM} : (a) 3 wt.%, (b) 6 wt.% and (c) 13 wt.%, were carried out during the exposure time $t_{irr} = 300$ s. Polymer networks were formed during exposure in Iso (solid squares), BPs (solid circles) and Ch (solid triangles). Thickness of the LC cells was 25.4 ± 0.5 μm . The cooling rate of the sample was $0.01^\circ\text{C}/\text{min}$.

cubic lattices), the temperature dependence of the broadening of ΔT_{BP} of BPs of PSCLCs, containing various C_{RMM} , was observed (Figure 15). As can be seen from Figure 15, the increase in T_{irr} gives rise to the increase in the temperature range ΔT_{BP} .

Conclusion

The influence of the photopolymerisation conditions, namely the temperature regime T_{irr} (or in other words the phase of the composite during the formation of the polymer networks) and UV exposure time t_{irr} , on the broadening of the temperature range ΔT_{BP} of the BPs was presented. It was shown that the changes of the photopolymerisation temperature T_{irr} (*i.e.* phase during UV exposure of the composite), exposure time t_{irr} of UV radiation and concentrations of RMM without any photoinitiators can be used to control the extension of the temperature range of BPs of PSCLCs, as summarised in Figures 5 and 15. Experimentally it is found that the extension of ΔT_{BP} is maximal, when photopolymerisation of the composite has been carried out in Iso over a prolonged exposure, and reaches the value 11.5°C, 16.5°C, 23.1°C and 24°C for $C_{RMM} = 3, 6, 10$ and 13 wt.%, respectively. The usage of PSCLCs with higher concentrations of RMM ($C_{RMM} = 10$ and 13 wt.%) is difficult owing to low optical characteristics (spectral broadening and increase in scattering), but temperature ranges ΔT_{BP} of BPs of these PSCLCs are wider. However, as shown in [55,58], the usage of various photoinitiators and monomers can increase amount of cross-linking chains and change the morphology of polymer networks that gives rise to a strong broadening of the temperature range ΔT_{BP} of BPs PSCLCs. As shown in Figure 15, the temperature T_{irr} , wherein polymer networks formed under UV exposure of PSCLCs in BPs, also should be taken into account to increase the temperature range of BPs of PSCLCs. Although composites described in this manuscript still have a narrow temperature range ΔT_{BP} of BPs compared to well-known BPs of PSCLCs, [16,17,28–33,42,55,58] here, the main goal was to demonstrate the influence of the different photopolymerisation conditions on the broadening of ΔT_{BP} and spectral characteristics of BP of PSCLCs.

Acknowledgements

Author I.G. thanks W. Becker (Merck) for his generous gift of chiral dopant R-811, Prof. I. Gerus (Institute of Bioorganic Chemistry and Petrochemistry, NAS of Ukraine) for the kind provision of polymers, Dr. S. Lukyanets (Institute of Physics, NAS of Ukraine), Prof. L. Lisetski

(Institute for Scintillation Materials of STC 'Institute for Single Crystals', NAS of Ukraine) and Prof. O. Lavrentovich (Kent State University, USA) for the some good advices and helpful discussions.

Disclosure statement

No potential conflict of interest was reported by the author.

References

- [1] Keyes PH, Nicastro J, McKinnon EM. Microscopic observations of the cholesteric blue phase in mixtures of varying pitch. *Mol Cryst Liq Cryst.* 1981;67:59–68. doi:10.1080/00268948108070875.
- [2] Marcus MA, Goodby JW. Cholesteric pitch and blue phases in a chiral-racemic mixture. *Mol Cryst Liq Cryst.* 1982;72:297–305. doi:10.1080/01406568208084724.
- [3] Meiboom S, Sammon M. Structure of the blue phase of a cholesteric liquid crystal. *Phys Rev Lett.* 1980;44:882–885. doi:10.1103/PhysRevLett.44.882.
- [4] Johnson DL, Flack JH, Crooker PP. Structure and properties of the cholesteric blue phases. *Phys Rev Lett.* 1980;45:641–644. doi:10.1103/PhysRevLett.45.641.
- [5] Meiboom S, Sammon M. Blue phases of cholesteryl nonanoate. *Phys Rev A.* 1981;24:468–475. doi:10.1103/PhysRevA.24.468.
- [6] Flack JH, Crooker PP. Polarization and pitch dependence of cholesteric blue-phase structures. *Phys Lett A.* 1981;82:247–250. doi:10.1016/0375-9601(81)90199-7.
- [7] Wright DC, Mermin D. Crystalline liquids: the blue phases. *Rev Mod Phys.* 1989;61:385–432. doi:10.1103/RevModPhys.61.385.
- [8] Belyakov VA, Dmitrienko VE. The blue phases of liquid crystals. *Sov Phys Usp.* 1985;28:535–562. doi:10.1070/pu1985v028n07abeh003870.
- [9] Crooker PP. Blue phases. In: Kitzerow H-S, Bahr C, editors. *Chirality of liquid crystals.* New York: Springer-Verlag; 2001. p. 186–222.
- [10] Kitzerow H-S. Blue phases of age: a review. In: Chien L-C, Wu MH, editors. *Emerging liquid crystal technologies IV.* Proceedings SPIE 7232. San Jose (CA). 2009 Jan 24. doi:10.1117/12.813372.
- [11] Henrich O, Stratford K, Cates ME, et al. Structure of blue phase III of cholesteric liquid crystals. *Phys Rev Lett.* 2011;106:107801-1-4. doi:10.1103/PhysRevLett.106.107801.
- [12] Bouligand Y, Lagerwall ST, Stebler B. Blue phase drops on a glass interface and their decoration at the cholesteric transition. *C R Chimie.* 2008;11:212–220. doi:10.1016/j.crci.2007.11.009.
- [13] Barbet-Massin R, Pieranski P. Optical properties of blue phase I: measurement of the order parameter. *J Phys Colloques.* 1985;46:C3-61-C3-78. doi:10.1051/jphyscol:1985306.
- [14] Lavrentovich OD, Kleman M. *Chirality in liquid crystals.* New York: Springer-Verlag; 2001.
- [15] Oswald P, Pieranski P. *Nematic and cholesteric liquid crystals: concepts and physical properties illustrated by experiments.* Boca Raton: CRC Press Taylor&Francis Group; 2005.

- [16] Kikuchi H, Yokota M, Hiskado Y, et al. Polymer-stabilized liquid crystal blue phases. *Nat Mater.* 2002;17:64–68. doi:10.1038/nmat712.
- [17] Hasson CD, Davis FJ, Mitchell GR. Imprinting chiral structures on liquid crystalline elastomers. *Chem Commun.* 1998;22:2515–2516. doi:10.1039/A805891A.
- [18] Jáklí A, Nair GG, Lee CK, et al. Macroscopic chirality of a liquid crystal from nonchiral molecules. *Phys Rev E.* 2001;63:061710-1-5. doi:10.1103/PhysRevE.63.061710.
- [19] Courty S, Tajbakhsh AR, Terentjev EM. Stereo-selective swelling of imprinted cholesteric networks. *Phys Rev Lett.* 2003;91:085503-1-4. doi:10.1103/PhysRevLett.91.085503.
- [20] Morris SM, Ford AD, Gillespie C, et al. The emission characteristics of liquid-crystal lasers. *J Soc Inf Display.* 2006;14:565–573. doi:10.1889/1.2210808.
- [21] Coles HJ, Pivnenko MN. Liquid crystal ‘blue phases’ with a wide temperature range. *Nature Lett.* 2005;436:997–1000. doi:10.1038/nature03932.
- [22] Park K-W, Gim M-J, Kim S, et al. Liquid-crystalline blue phase II system comprising a bent-core molecule with a wide stable temperature range. *Appl Mater Interfaces.* 2013;5:8025–8029. doi:10.1021/am403109q.
- [23] Yoshizawa A, Sato M, Rokunohe J. A blue phase observed for a novel chiral compound possessing molecular biaxiality. *J Mater Chem.* 2005;15:3285–3290. doi:10.1039/B506167A.
- [24] Wang H, Zheng Z, Shen D. Blue phase liquid crystals induced by bent-shaped molecules based on 1,3,4-oxadiazole derivatives. *Liq Cryst.* 2012;39:99–103. doi:10.1080/02678292.2011.628704.
- [25] Lin T-H, Li Y, Wang C-T, et al. Red, green and blue reflections enabled in an optically tunable self-organized 3D cubic nanostructured thin film. *Adv Mater.* 2013;25:5050–5054. doi:10.1002/adma.201300798.
- [26] Xiang J, Lavrentovich OD. Blue-phase-polymer-templated nematic with sub-millisecond broad-temperature range electro-optic switching. *Appl Phys Lett.* 2013;103:051112-1-4. doi:10.1063/1.4817724.
- [27] Castles F, Day FD, Morris SM, et al. Blue-phase templated fabrication of three-dimensional nanostructures for photonic applications. *Nature Mater.* 2012;11:599–603. doi:10.1038/nmat3330.
- [28] Bobrovsky A, Boiko NI, Shibaev VP. Phase diagrams and optical properties of new menthyl-containing LC copolymers forming chiral mesophases. *Liq Cryst.* 1998;24:489–500. doi:10.1080/026782998206948.
- [29] Kikuchi H, Izena S, Higuchi H, et al. A giant polymer lattice in a polymer-stabilized blue phase liquid crystal. *Soft Matter.* 2015;11:4572–4575. doi:10.1039/C5SM00711A.
- [30] Choi H, Higuchi H, Ogawa Y, et al. Polymer-stabilized supercooled blue phase. *Appl Phys Lett.* 2012;101:131904-1-5. doi:10.1063/1.4752461.
- [31] Kasch N, Dierking I, Turner M. Stabilization of the liquid crystalline blue phase by the addition of short-chain polystyrene. *Soft Mater.* 2013;9:4789–4793. doi:10.1039/c3sm00065f.
- [32] Castles F, Morris SM, Hung JMC, et al. Stretchable liquid-crystal blue-phase gels. *Nat Mater.* 2014;13:817–821. doi:10.1038/NMAT3993.
- [33] Nordendorf G, Hoischen A, Schmidtke J, et al. Polymer-stabilized blue phases: promising mesophases for a new generation of liquid crystal displays. *Pol Adv Technol.* 2014;25:1195–1207. doi:10.1002/pat.3403.
- [34] Zheng Z, Shen D, Huang P. Wide blue phase range of chiral nematic liquid crystal doped with bent-shaped molecules. *New J Phys.* 2010;10:113018-1-10. doi:10.1088/1367-2630/12/11/113018.
- [35] Cordoyiannis G, Losada-Pérez P, Shekhar Pati Tripathi C, et al. Blue phase III widening in CE6-dispersed surface-functionalised CdSe nanoparticles. *Liq Cryst.* 2010;37:1419–1426. doi:10.1080/02678292.2010.519057.
- [36] Karatairi E, Rožič B, Kutnjak Z, et al. Nanoparticle-induced widening of the temperature range of liquid-crystalline blue phases. *Phys Rev E.* 2010;81:041703-1-5. doi:10.1103/PhysRevE.81.041703.
- [37] Yoshizawa A. Material design for blue phase liquid crystals and their electro-optical effects. *RSC Adv.* 2013;3:25475–25497. doi:10.1039/c3ra43546f.
- [38] Pawsey AC, Clegg PS. Colloidal particles in blue phase liquid crystals. *Soft Mater.* 2015;11:3304–3312. doi:10.1039/C4SM02131B.
- [39] Fukuda JI. Stabilization of a blue phase by a guest component: an approach based on a Landau-de Gennes theory. *Phys Rev E.* 2010;82:061702-1-5. doi:10.1103/PhysRevE.82.061702.
- [40] Fukuda JI. Stability of cholesteric blue phase in the presence of a guest component. *Phys Rev E.* 2012;86:041704-1-6. doi:10.1103/PhysRevE.86.041704.
- [41] Fukuda J, Žumer S. Field-induced dynamics and structures in a cholesteric-blue-phase cell. *Phys Rev E.* 2013;87:042506-1-12. doi:10.1103/PhysRevE.87.042506.
- [42] Hirose T, Yoshizawa A. Comparison of electro-optical switching between polymer-stabilised cubic and amorphous blue phases. *Liq Cryst.* 2015;42:1290–1297. doi:10.1080/02678292.2015.1048755.
- [43] Coles H, Morris S. Liquid-crystal lasers. *Nature Photonics.* 2010;4:676–685. doi:10.1038/nphoton.2010.184.
- [44] Cao W, Muñoz A, Palffy-Muhoray P, et al. Lasing in a three-dimensional photonic crystal of the liquid crystalline blue phase II. *Nature Mater.* 2002;1:111–113. doi:10.1038/nmat727.
- [45] Yokoyama S, Mashiko S, Kikuchi H, et al. Laser emission from a polymer-stabilized liquid-crystalline blue phase. *Adv Mater.* 2006;18:48–51. doi:10.1002/adma.200501355.
- [46] Yan J, Li Y, Wu S-T. High efficiency and fast-response tunable grating using a blue phase liquid crystal. *Opt Lett.* 2011;36:1404–1406. doi:10.1364/OL.36.001404.
- [47] Ge Z, Gauza S, Jiao M, et al. Electro-optics of polymer-stabilized blue phase liquid crystal displays. *Appl Phys Lett.* 2009;94:101104. doi:10.1063/1.3097355.
- [48] Jiao M, Li Y, Wu S-T. Low voltage and high transmittance blue-phases liquid crystal displays with corrugated electrodes. *Appl Phys Lett.* 2010;96:011102-1-3. doi:10.1063/1.3290253.
- [49] Rao L, Ge Z, Wu S-T, et al. Low voltage blue-phases liquid crystal displays. *Appl Phys Lett.* 2009;95:231101-1-3. doi:10.1063/1.3271771.
- [50] Lu SY, Chein LC. Electrically switched color with polymer-stabilized blue-phase liquid crystals. *Opt Lett.* 2010;35:562–564. doi:10.1364/OL.35.000562.
- [51] Yan J, Rao L, Jiao M, et al. Polymer-stabilized optically isotropic liquid crystals for next-generation display and

- photonics applications. *J Mater Chem.* 2011;21:7870–7877. doi:10.1039/C1JM10711A.
- [52] Haseba Y, Kikuchi H. Optically isotropic chiral liquid crystals induced by polymer network and their electro-optical behaviour. *Mol Cryst Liq Cryst.* 2007;470:1–9. doi:10.1080/15421400701490535.
- [53] Liu Y, Xu S, Xu D, et al. A hysteresis-free polymer-stabilised blue-phase liquid crystal. *Liq Cryst.* 2014;41:1339–1344. doi:10.1080/02678292.2014.920055.
- [54] Zhu J-L, Ni S-B, Chen CP, et al. The influence of polymer system on polymer-stabilised blue phase liquid crystals. *Liq Cryst.* 2014;41:891–896. doi:10.1080/02678292.2014.882023.
- [55] Iwata T, Takaoka T, Suzuki K, et al. The influence of thermal property of the polymer on the polymer-stabilised blue phase. *Mol Cryst Liq Cryst.* 2007;470:11–18. doi:10.1080/15421400701492374.
- [56] Ni S-B, Zhu J-L, Tan J, et al. Critical temperature in phase transition of blue phase liquid crystal. *Opt Mater Express.* 2013;3:928–934. doi:10.1364/OME.3.000928.
- [57] Yan J, Wu S-T. Effect of polymer concentration and composition on blue phase liquid crystals. *J Display Tech.* 2011;7:490–493. doi:10.1109/JDT.2011.2159091.
- [58] Chen H-Y, Wu C-K, Chen F-C, et al. Investigation on morphology of polymer structure in polymer-stabilized blue phase. *Liq Cryst.* 2016. doi:10.1080/02678292.2016/1173244.
- [59] Gvozдовskyy I. ‘Blue phases’ of highly chiral thermotropic liquid crystals with a wide range of near-room temperature. *Liq Cryst.* 2015;42:1391–1404. doi:10.1080/02678292.2015.1053001.
- [60] Bae KS, Kim M, Yu CJ, et al. White reflection film by photopolymerization of reactive mesogen in cholesteric liquid crystal layer. *IMID Digest.* 2012;771–772.
- [61] Duning MM Processing-structure-property relationships of a polymer-templated cholesteric liquid crystal exhibiting dynamic selective reflection [M.S. thesis]. Dayton: The school of engineering of the University of Dayton; 2012.